American Mineralogist, Volume 97, pages 890–896, 2012

The dual behavior of the β-As_4S_4 altered by light

MATTEO ZOPPI[1,2]* AND GIOVANNI PRATESI[1,3]

[1]Museo di Storia Naturale, Sezione di Mineralogia, Università di Firenze, via La Pira 4, I-50121 Firenze, Italy
[2]Museo di Scienze Planetarie, Provincia di Prato, via Galcianese 20/H, I-59100 Prato, Italy
[3]Dipartimento di Scienze della Terra, Università di Firenze, via La Pira 4, I-50121 Firenze, Italy

ABSTRACT

Among the polymorphs of the compound As_4S_4, realgar and β-As_4S_4 exhibit an interesting phenomenon of light-induced alteration that eventually leads to the transformation to pararealgar and arsenolite through the structural modification of the As_4S_4 molecule. The mechanism generally invoked to explain the transformation assumes reaction with oxygen, subsequent modification of the molecule through an insertion of a sulfur atom and the eventual production of arsenolite according to the reaction $5As_4S_4 + 3O_2 \rightarrow 4As_4S_5 + 2As_2O_3$. Early studies showed that the light-induced transition from realgar to pararealgar is reversible through heat and that implies a transition through the χ-phase, even though the presence of arsenolite was not observed. To further assess the action of the oxygen during the process, we carried out experiments of light-induced alteration of β-As_4S_4 under ambient air and under isopropyl alcohol. The material was investigated by means of X-ray powder diffraction (XRPD) using quantitative phase analysis (QPA) and the Rietveld method. The further study of the heat-induced transformation of the products showed that β-As_4S_4 exhibits a dual behavior: if the light-induced alteration occurs under air, arsenolite plus an amorphous phase is produced and the transformation is not reversible, if the alteration occurs without any contact to air none of such phases is produced and the transformation is reversible. These new experimental evidences suggest that the production of arsenolite is not strictly required for the transformation of the β-As_4S_4 into pararealgar and that the current model invoked to explain the mechanism of alteration should be modified to take into account the dual behavior of the β-As_4S_4 altered by light.

Keywords: β-As_4S_4, light, heat, pararealgar, alacranite, Rietveld

INTRODUCTION

Although interaction of light with minerals forms the foundation of many optical properties, very few mineral species show permanent transformations due to visible radiation. One prominent example is the mineral realgar (α-As_4S_4), and its high-temperature polymorph, β-As_4S_4. Both undergo a peculiar process of alteration induced by light. Curiously these materials have also been used as orange pigments by artists through different ages, from ancient Egypt to the Middle Ages and the Renaissance, and this alteration might have implications regarding the study, interpretation, and conservation of antique paintings (Corbeil and Helwig 1995; Trentelman et al. 1996; Clark and Gibbs 1997, 1998; Burgio et al. 2003, 2006). The light-induced alteration causes a change of the beautiful orange color of realgar to the yellow color of pararealgar. This process is highly interesting from a structural point of view. There are four polymorphs of As_4S_4.Their structure differs in the type of molecules and their packing in the unit cell ($Z = 4$) due to van der Waals forces. Realgar (space group $P2_1/n$) has been described as a regular packing of cage-like molecules (Fig. 1a) where each As atom is covalently bonded to two S and one As atoms, and each S atom is bonded to two As atoms (Ito et al. 1952; Street and Munir 1970; Mullen and Nowacki 1972). A different packing of the same molecular unit leads to the β-phase (β-As_4S_4, space group $C2/c$) (Porter and Sheldrick 1972), which is stable up to 252 °C (Roland 1972) and metastable at room temperature. Both polymorphs alter to pararealgar (Bonazzi et al. 1995), as a result of exposure to natural or artificial light (Douglass et al. 1992; Bonazzi et al. 1996). In the molecular unit of As_4S_4 pararealgar (Fig. 1b), one As atom is covalently bonded to one S and two As atoms, two As atoms are bonded to one As and two S atoms, while one As atom is bonded to

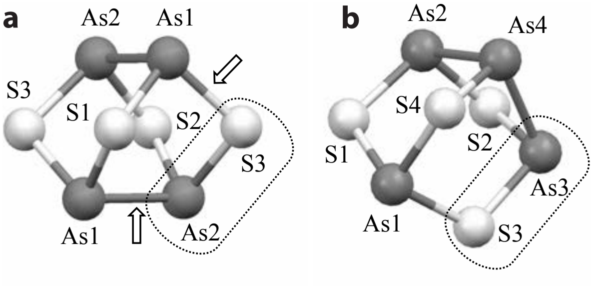

FIGURE 1. The molecules of realgar and β-As_4S_4 (**a**), and pararealgar and As_4S_4(II) (**b**). The arrows point to the bonds to be broken, and the outlined area includes the fragment that is displaced for the molecule of the first two polymorphs to transform to that of pararealgar. The atom labels correspond to those used in the literature.

---

* E-mail: matteo.zoppi@unifi.it

0003-004X/12/0506–890$05.00/DOI: http://dx.doi.org/10.2138/am.2012.3968

three S atoms. Each S atom is bonded to two As atoms. This cradle-like molecule can be arranged in two different kinds of packing, that of pararealgar ($P2_1/c$), and the one of a synthetically obtained phase, named As_4S_4(II), whose space group is $P2_1/n$ (Kutoglu 1976). The transformation of the molecule of α and β polymorphs to that of pararealgar implies the breaking of one As-As and one As-S bond. As observed since the study of Douglass et al. (1992), the action of visible light causes an anisotropic increase of the unit-cell volume (up to 2.6%) of both the α and β polymorphs, and during the process of alteration a metastable phase occurs, named χ-phase, which is the precursor of pararealgar. Arsenolite (As_2O_3) was reported to form starting from both realgar (Ballirano and Maras 2006) and from β-As_4S_4 (Zoppi 1998), and this phenomenon seems to be the result of the breaking of As-As and As-S bonds and the presence of oxygen.

Remarkable work has been done to understand the nature of the transformation and the structural modifications that occur within the different poymorphs (Douglass et al. 1992; Muniz-Miranda et al. 1996; Bonazzi et al. 2006; Bonazzi and Bindi 2008), regarding different species (Bindi et al. 2003; Bonazzi et al. 2003a; Bindi and Bonazzi 2007) and with different conditions of illumination (Kyono 2007; Naumov et al. 2007). Previous experimental work aimed to investigating the role of the oxygen during the process has been carried out by us starting from powdered β-As_4S_4 not in contact with air. The alteration proceeded until the complete transformation to pararealgar without any detectable presence of arsenolite. That suggests that the molecule of realgar (*R*-type) can transform to the one of pararealgar (*P*-type) even without the direct contact of the oxygen. An open question on the sudden transformation from *R* to *P* molecule in the presence of oxygen to form arsenolite is the fate of the released sulfur atoms. This question is still valid in the light of the model proposed by Kyono et al. (2005), based on the hypothesis of Bindi et al. (2003). The authors relate the unit-cell expansion to the substitution of As_4S_4 units by As_4S_5 uzonite-type molecules according to the reaction $5As_4S_4 + 3O_2 \rightarrow 4As_4S_5 + 2As_2O_3$, and the subsequent removal of the additional sulfur atom to produce the pararealgar molecule. Thus, the untied S atom would be ready to enter another realgar molecule and continue the cyclic mechanism. The assumption of the coexistence of As_4S_4 and As_4S_5 molecules within the unit-cell of realgar seemed to be confirmed by the observation of their simultaneous presence in the mineral alacranite (Bonazzi et al. 2003a, 2003b). Furthermore, alacranite (belonging to the series β-As_4S_4-As_8S_9) undergoes a light-induced volume expansion that is proportional to the percentage of the As_4S_5 molecules formed during the alteration (Bonazzi et al. 2006). The authors ascribe the structural changes of realgar, alacranite, and β-As_4S_4 to the disordered replacement of some As_4S_4 units by As_4S_5 molecules, according to the suggested reaction. Again, during the process leading to the complete transformation to pararealgar there would be some sulfur liberated by the As_4S_5 molecule. To the present time, no author made a hypothesis whether these sulfur atoms might be still present in some form within the altered material or escape as a gas. Another question concerns the phases formed from β-As_4S_4 during the alteration process. We observed that in the presence of air pararealgar and arsenolite crystallize, while only pararealgar is found as product under anoxic conditions. Is the difference to be only ascribed to the presence of arsenolite?

A different perspective of the problem might arise when considering the reverse transformation from pararealgar to β-As_4S_4 and realgar. The modification of the As_4S_4 molecule typical for pararealgar and As_4S_4-(II), to the molecule of the β-As_4S_4 and realgar is possible and occurs simply through the action of heat (Douglass et al. 1992). Although only little attention has been given to implications of the reverse transformation, the authors showed that natural pararealgar, sealed in a silica vial, transformed to β-As_4S_4 within 5 min at a temperature of 300 °C (in the β-As_4S_4 field), while the transformation was slower at a temperature of 220 °C, i.e., in the realgar stability field. At even lower temperatures (195 and 175 °C), the pararealgar transformed first to χ-phase, then to β-As_4S_4 and eventually to realgar. These results are surprising since β-As_4S_4 occurs below the $\alpha \rightarrow \beta$ transformation temperature. They also show that the χ-phase occurs in the reverse transformation from pararealgar to β-As_4S_4.

We collected XRPD data from samples of pararealgar obtained by completely altering some β-As_4S_4 powder with and without the presence of the air, as well as after the materials have been thermally treated, and the results are noteworthy.

The study of a multistage reverse transformation, from pararealgar to β-As_4S_4 and realgar might lead to a better understanding of the light-induced structural modifications of the pararealgar and realgar molecules and of the dynamics of the process. As a result this could bring potential applications in the field of opto-electronics, in the restoration of artwork damaged by the action of the light, as well as in medicine, where the use of realgar is proven to be effective for the treatment of various forms of cancer in vitro and in vivo (Lu et al. 2002; Zhao et al. 2009).

EXPERIMENTAL METHODS AND RIETVELD REFINEMENTS

The material used for this study (specimen no. 46768, Museo di Mineralogia dell' Università degli Studi di Firenze), is an aggregate of large crystals of realgar from the locality of Shimen, Hunan Province, China. The mineral is of high purity with minor traces of Sb as confirmed by the formula $(As_{0.9997}Sb_{0.0013})_{\Sigma=1.0010}S$ based on chemical analyses of samples from this locality (Xiong and Liu 1998). Some fragments of the unaltered crystalline realgar were carefully ground in an agate mortar under acetone; all the operations of manipulation of the sample were carried out in the dark, to avoid alteration. The β-As_4S_4 was obtained by placing some powdered realgar in an evacuated silica vial, kept at 290 °C in a horizontal furnace for 4 h, then quenched in water to 0 °C, and ground again. Half of the β-As_4S_4 powder was sealed in a transparent glass vial containing pure isopropyl alcohol, and the other half was spread on a white porcelain mortar to ensure contact with ambient air. The light-induced alteration of the two samples of β-As_4S_4 was obtained by means of an electronic apparatus (Schott KL 1500) equipped with a Philips dichroic halogen lamp and two optical fibers. The complete alteration of the β-As_4S_4 to pararealgar was obtained by exposing both the materials for about 300 h to light, while frequently stirring the powder. The altered material was placed in a nitrogen-purged glove box, ground and dried, and finally packed and sealed into 0.5 mm diameter glass capillaries. A total of four samples were prepared: the one labeled A, using the powdered β-As_4S_4 altered under air; the one labeled B, using the powdered β-As_4S_4 altered in isopropyl alcohol; and those labeled C and D were prepared with the same material used for samples A and B, respectively, with the addition of 12 wt% of yttrium-III oxide (analytical grade) used as internal standard to perform quantitative phase analysis (QPA). For all samples, thermal treatment was carried out in a furnace at a constant temperature of 220 °C for a total of 1, 24, 72, and 264 h, with air quenching the samples after each heating cycle. For samples C and D, XRPD data collections were carried out at each step, and labeled accordingly, adding the suffix 1, 24, 72, and 264. For samples A and B, data collections were carried out only after the last thermal treatment (at 264 h). XRPD data were collected using a Panalytical XPert-Pro diffractometer (Cu*K*α radiation at 40 KV, 40 mA) equipped with a focusing mirror, a goniometer (PW3050/60) with θ-θ geometry, a PIXcel (Medipix2) solid-state detector (de Vries et al. 2007), and a capillary spinner. On the incident beam a Soller slit (0.04 rad) and a divergence slit (¼°) were mounted, on the diffracted beam an antiscatter slit (7.50 mm) and a Soller slit (0.04 rad) were mounted. The setting employed for the data collections used for the structure refinements (samples A and B) was the following: 2θ range of 8–120°, step size of 0.01313°, common counting time (not step time) of 300 s, for a total time of 2:51 h. The setting employed for the data collections used for the QPA (samples C and D) was the following: 2θ range of 10–110°, step size of 0.02626°, common counting time of 118 s, for a total time of 30 min. For assessing the error resulting from QPA, performed with the latter experimental conditions, four samples of pure crystalline realgar were finely grounded, adding 4, 8, 12, and 16 wt% of internal standard, and the powder was sealed in glass capillaries. XRPD data collections were labeled R4, R8, R12, and R16, respectively.

Multiphase Rietveld refinements of the structural parameters were performed with the GSAS software (Larson and Von Dreele 2004), using the graphical user interface EXPGUI (Toby 2001). The following items were modeled by refining the corresponding parameters: background contribution (using a Chebyshev polynomial with a variable number of terms), scale factors, lattice parameters, Lorentzian and Gaussian terms of the pseudo-Voigt peak-shape model, microstrain line broadening parameters (Stephens 1999), atomic positions and isotropic atomic displacement parameters. The starting structural models, for the phases to be refined, have been taken from literature. Damping factors were always applied, especially in the first stages of refinements. QPA was performed applying the Rietveld-RIR method (Gualtieri 2000) and refining the structural parameters of the phases occurring in the samples.

INTERPRETATION OF XRD PATTERNS AND QPA RESULTS

The relative error percent as obtained from the QPA refinements performed on samples R4, R8, R12, and R16 are shown in the histogram of Figure 2. It is clear that the lowest error percentage is obtained from the sample R16 but, if compared with the sample R12, the difference is small. An amount of yttrium-III oxide higher or equal to 12% by weight yields diffraction peaks sufficiently resolved to allow an accurate quantification of the phases. We have chosen to add 12 wt% of internal standard for performing the QPA on samples C and D, because this is the smallest amount necessary to minimize the problem of peak overlapping while still yielding an accurate quantification of the As_4S_4 polymorphs. The use of realgar for this purpose is justified by the fact that all the polymorphs of the As_4S_4 have, with a good approximation, the same X-ray linear absorption coefficient, and that the realgar used has not been treated, nor obtained synthetically.

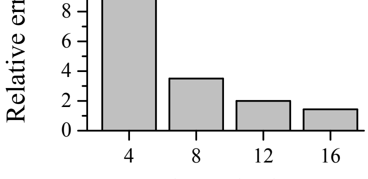

FIGURE 2. The relative error percent as obtained from the refinements for the QPA performed on samples R4, R8, R12, and R16.

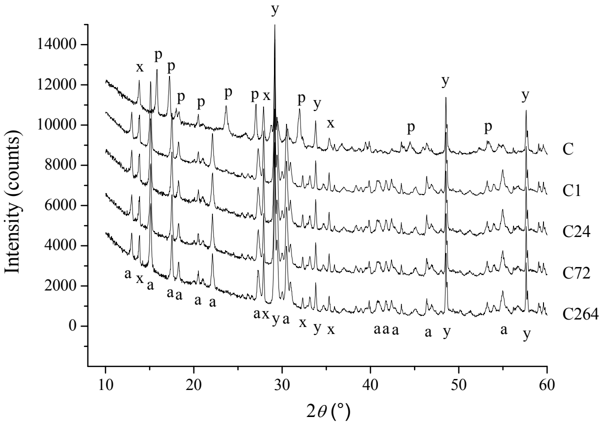

FIGURE 3. XRPD patterns, shown in the range 10–60 °2θ, as collected from sample C. The main peaks of pararealgar (p), arsenolite (x), alacranite (a) and yttrium-III oxide (y) are labeled.

XRPD patterns collected before and after the various stages of thermal treatment of samples C and D are shown in the Figures 3 and 4, respectively. The data show that, from the alteration of the β-As_4S_4 performed in the presence of air (sample C), pararealgar and arsenolite were obtained, and from the alteration of the same material, carried out under isopropyl alcohol (sample D), only pararealgar was obtained. The treatments performed through the annealing at 220 °C showed very interesting results. From sample C, arsenolite and alacranite crystallized, while from sample D initially an expanded form of β-As_4S_4, identified as the χ-phase, and eventually the β-As_4S_4 crystallized. Furthermore, the QPA let us detect a significant amount of amorphous material in sample C after the light-induced alteration, which was not the case in sample D. The weight percent of the phases detected in samples C and D after light-induced alteration and after each stage of the thermal treatment is reported in Table 1, and for the phases of sample C the molar ratio, with respect to two moles of the arsenolite, has been calculated. This is useful for comparing the molar ratios with those of the reaction mentioned in previous work (Bindi et al. 2003; Kyono et al. 2005). The chemical formula of the amorphous phase is expected to be AsS_2, as explained further down, and the relative weight of it is 14.82%. For the light-induced alteration stage, the calculated weight percent of the amorphous phase as obtained by the Rietveld-RIR method is very low (0.66%) in sample D and can therefore be considered zero. In fact this value represents the error on the quantification of pararealgar, which in terms of relative error is lower than 2%. The same explanation applies to the partly negative weight percent values reported for the amorphous phase in samples C and D. The results of the experiments are summarized in Figure 5, and it is worth noting that during the light-induced alteration of the β-As_4S_4 to pararealgar under isopropyl alcohol, no arsenolite or amorphous phase was detected. Results of Rietveld refinements of patterns from samples A and B with the aim of characterizing alacranite as well as β-As_4S_4 formed during the heat-induced transformation of pararealgar are shown in Figures 6 and 7, and Table 2, respectively. For alacranite, which

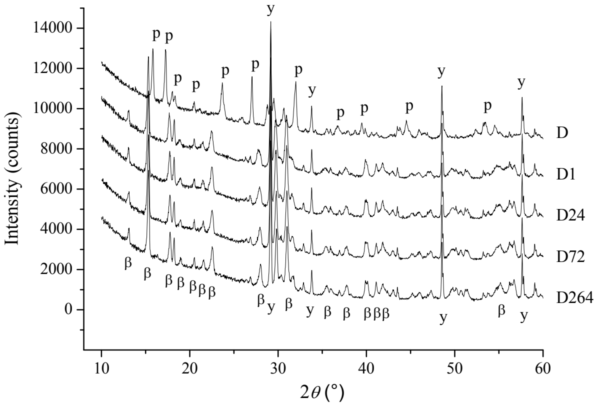

FIGURE 4. XRPD patterns, shown in the range 10–60 °2θ, as collected from sample D. The main peaks of pararealgar (p), β-As_4S_4 (β) and yttrium-III oxide (y) are labeled.

was formed during the last stage of the thermal treatment, the fractional atomic coordinates and thermal parameters are reported in Table 3, while the interatomic bond distances and angles are shown in Table 4. The respective values for β-As_4S_4 are reported in Tables 5 and 6. CIFs are available on deposit[1].

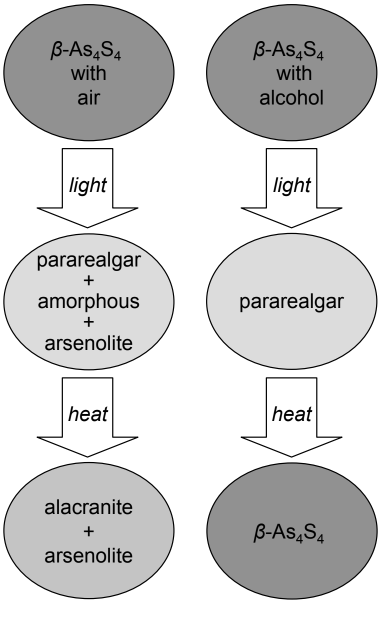

FIGURE 5. Diagram showing the transformation of the β-As_4S_4 in the presence of ambient air (**left**) and under isopropyl alcohol (**right**). The alteration was first induced by light then by heat (see text).

DISCUSSION

The plan of this work was to study the light-induced alteration of β-As_4S_4 under two different conditions, namely with and without presence of air (i.e., oxygen). The experiment under isopropyl alcohol had the purpose of preventing the contact with oxygen, although this might still occur in a very low concentration in the alcohol, and a catalytic reaction involving the β-As_4S_4 molecules cannot be ruled out. The main result is that the two different conditions of the light-induced alteration led to different results. If exposed to light under air, β-As_4S_4 transformed to pararealgar, arsenolite, and an amorphous phase, while under isopropyl alcohol all of the β-As_4S_4 transformed to pararealgar. The current model proposed for the expansion of the unit-cell of realgar (Bindi et al. 2003; Kyono et al. 2005) and the reaction $5As_4S_4 + 3O_2 \rightarrow 4As_4S_5 + 2As_2O_3$ do not explain the presence of the amorphous phase produced during the transformation of the β-As_4S_4. In the anoxic case (sample D), assuming a catalytic role of sulfur atoms in order to transform the β-As_4S_4 molecules into the ones of pararealgar, arsenolite cannot be formed as a reaction product, and the occurrence of the unit-cell expansion remains unexplained. In the light-induced alteration taking place under air (sample C), it is possible to write a reaction such as the following:

$$9As_4S_4 + 3O_2 \rightarrow 7As_4S_4 + 4AsS_2 + 2As_2O_3$$

where the values of the molar ratios (Table 1) are given by to the formula unit. Thereby, the chemical composition the amorphous phase (AsS_2) is given by the necessity to balance the reaction. Furthermore, the thermal treatment shows that the process of light-induced alteration occurring under air is not reversible by heating the sample, whereas the transformation under exclusion of air seems to be reversible. From the results of the QPA for sample C (Table 1), we find that the amount of arsenolite remains roughly the same from the beginning of the heat-induced alteration through all annealing stages of 1,

TABLE 1. Weight percent of phases in samples C and D, after light-induced alteration after each stage of thermal treatment, together with the calculated molar ratios for arsenolite, as derived from the QPA carried out with the Rietveld-RIR method

		Light-induced alteration		Thermal treatments							
				1		24		72		264	
		wt%	ratio	wt%	ratio	wt%	ratio	wt%	ratio	wt%	ratio
sample C	pararealgar	75.18	6.95	–	–	–	–	–	–	–	–
	arsenolite	10.00	2	9.53	2	9.74	2	9.25	2	9.35	2
	alacranite	–	–	90.66	4.24	91.12	4.17	90.56	4.36	91.13	4.35
	amorphous*	14.82	4.22	–0.19	–0.06	–0.86	–0.25	0.19	0.06	–0.48	–0.14
sample D	pararealgar	99.34		–		–		–		–	
	β-As_4S_4	–		99.91		101.05		99.15		98.41	
	amorphous	0.66		0.09		–1.05		0.85		1.59	

* The molar ratio has been calculated based on the formula AsS_2.

---

[1] Deposit item AM-12-028, CIFs. Deposit items are available two ways: For a paper copy contact the Business Office of the Mineralogical Society of America (see inside front cover of recent issue) for price information. For an electronic copy visit the MSA web site at http://www.minsocam.org, go to the *American Mineralogist* Contents, find the table of contents for the specific volume/issue wanted, and then click on the deposit link there.

24, 72, and 264 h, respectively. Pararealgar and the amorphous phase completely disappear in favor of the crystallization of alacranite during the first heating stage. Its weight percent remains constant throughout the heating process. The following reaction is proposed in accordance with the measured molar ratios of alacranite and arsenolite:

$$7As_4S_4 + 4AsS_2 + 2As_2O_3 \rightarrow 4As_8S_9 + 2As_2O_3.$$

From a structural point of view, alacranite, which was formed by heat-induced transformation (Tables 2, 3, and 4), matches the natural alacranite described by Bonazzi et al. (2003b), even though little differences are present. The unit-cell volume is 1.44% smaller than that reported by Bonazzi et al. (2003b) (844.8 vs. 857.1 Å³); also some of the interatomic bond distances in the As_4S_4 molecule differ slightly. Similar minor discrepancies between this study and the one of Bonazzi et al. (2003b) are found for the As_4S_5 molecule. Also interatomic bond angles in the As_4S_4 molecule exhibit a slightly smaller value (S1-As1-S3*) and some slightly higher values (As1-S1-As1*, As2-S2-As2*). Similar variations are also reported for other nonstoichiometric types of alacranites (Bonazzi et al. 2003a 2006) and can be due to some local disordered distribution of As_4S_4 and As_4S_5 molecules. In this case, given the similar topology of the two molecules, the refined atomic coordinates would represent average values of the positions occupied by analogous atoms belonging to the As_4S_4 and As_4S_5 molecules, respectively.

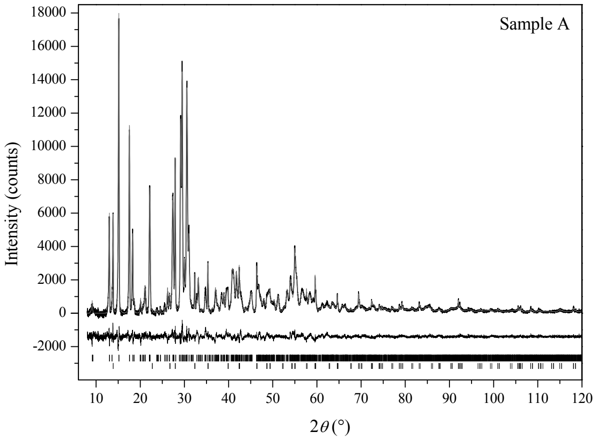

FIGURE 6. Background subtracted diffraction pattern of sample A. From top to bottom: observed, calculated, residual pattern, and reflections positions for alacranite and arsenolite are reported.

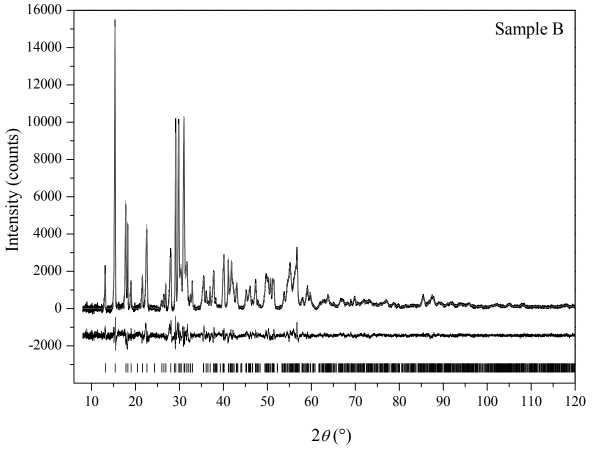

FIGURE 7. Background subtracted diffraction pattern of sample B. From top to bottom: observed, calculated, residual pattern, and β-As_4S_4 reflections positions are reported.

TABLE 2. Residual indices of Rietveld refinements, as defined in GSAS (Larson and Von Dreele 2004) and unit-cell parameters for alacranite (sample A) and β-As_4S_4 (sample B)

Alacranite	
R_{wp} = 2.85%	a = 9.9342(6) Å
R_p = 2.06%	b = 9.5566(6) Å
χ^2 = 2.76	c = 9.1104(5) Å
$R(F^2)$ = 4.89%	β = 102.397(2)°
$R(F)$ = 2.65%	V = 844.8(1) Å³
β-As_4S_4	
R_{wp} = 3.49%	a = 9.967(1) Å
R_p = 2.49%	b = 9.355(1) Å
χ^2 = 3.63	c = 8.921(1) Å
$R(F^2)$ = 4.63%	β = 102.520(2)°
$R(F)$ = 2.58%	V = 812.0(3) Å³

TABLE 3. Fractional atomic coordinates and isotropic thermal parameters for alacranite (sample A)

	x/a	y/b	z/c	U_{iso}
As1	0.0186(4)	0.2190(4)	0.9450(4)	0.051(1)
As2	0.1656(4)	0.4255(5)	0.8627(5)	0.055(2)
As3	0.4589(4)	0.3154(5)	0.4367(5)	0.086(2)
As4	0.3712(4)	0.0359(4)	0.1793(6)	0.060(2)
S1	0	0.0944(14)	3/4	0.018(4)
S2	0	0.5482(12)	3/4	0.032(4)
S3	0.1961(6)	0.3162(7)	0.6489(8)	0.015(2)
S4	0.2837(6)	0.1733(8)	0.3259(9)	0.030(3)
S5	1/2	0.4385(11)	1/4	0.020(4)
S6	0.3833(7)	0.1725(8)	–0.0023(9)	0.048(3)

TABLE 4. Interatomic bond distances (Å) and angles (°) for alacranite (sample A)

As_4S_4 molecule		As_4S_5 molecule	
Intramolecular bond distances			
As1-S1	2.113(8)	As3-S6†	2.069(7)
As1-S3*	2.316(7)	As3-S5	2.177(7)
As1-As2	2.657(6)	As3-S4	2.267(8)
As2-S2	2.100(8)	As4-S6	2.130(9)
As2-S3	2.287(8)	As4-S4	2.182(9)
As2-As1	2.657(6)	As4-As4†	2.606(8)
Intramolecular bond angles			
S1-As1-S3*	90.5(3)	S4-As3-S5	103.4(3)
S1-As1-As2	97.8(3)	S4-As3-S6†	101.2(3)
S3-As1-As2	96.7(2)	S5-As3-S6†	109.0(4)
S3-As2-S2	94.1(3)	As4-As4-S6	99.9(3)
S3-As2-As1	94.7(3)	S4-As4-As4†	100.1(3)
S2-As2-As1	97.6(3)	S6-As4-S4†	101.7(3)
As1-S1-As1*	111.5(7)	As3-S4-As4	105.3(3)
As2-S2-As2*	112.1(6)	As3-S5-As3†	114.6(6)
As2-S3-As1*	102.6(3)	As4-S6-As3†	110.2(4)

Note: Symmetry codes: * = –x, y, 3/2–z; † = 1–x, y, 1/2–z.

TABLE 5. Fractional atomic coordinates and isotropic thermal parameters for β-As_4S_4 (sample B)

	x/a	y/b	z/c	U_{iso}
As1	0.0003(2)	–0.2049(2)	0.0553(2)	0.049(1)
As2	–0.1579(2)	–0.4037(2)	0.1308(3)	0.042(1)
S1	0	–0.0599(6)	1/4	0.032(2)
S2	0	–0.5501(7)	1/4	0.061(2)
S3	–0.2026(3)	–0.3057(4)	0.3377(5)	0.035(2)

TABLE 6. Interatomic bond distances (Å) and angles (°) for β-As_4S_4 (sample B)

Intramolecular bond distances	
As1_S1	2.204(3)
As1_S3	2.243(4)
As1_As2	2.619(2)
As2_S2	2.181(5)
As2_S3	2.191(5)
Intramolecular bond angles	
S1-As1-S3	94.5(1)
S1-As1-As2	97.5(1)
S3-As1-As2	97.3(1)
S3-As2-S2	96.3(2)
S3-As2-As1	99.4(1)
S2-As2-As1	99.2(1)
As1-S1-As1	104.0(3)
As2-S2-As2	102.2(3)
As1-S3-As2	101.9(2)

This could also explain the slightly higher isotropic thermal parameters shown by some atoms of alacranite. Some remarks should be made about the nature of the amorphous phase formed during the alteration. Its composition is deduced as AsS_2 from the need to balance the reaction. Whether it is a single amorphous phase or a mixture of two or more amorphous phases cannot be decided based on the present experiment, however the existence and the nature of a chalcogenide glass of chemical formula $As_{0.33}S_{0.67}$ has been well documented (Wágner et al. 2003; Krbal et al. 2007; Hasapis et al. 2010; Kaban et al. 2011). This amorphous phase is the starting material for the $Ag_x(As_{0.33}S_{0.67})_{100-x}$ bulk glasses ($0 \leq x \leq 28$) studied for the interesting property of persistent photo-generated voltage for which it is used in solid-state photochemical cells. The authors point out that the network of the chalcogenide glass $As_{0.33}S_{0.67}$ is based on chains of corner-sharing AsS_3 pyramidal units, the same building blocks found in many arsenic sulfides.

The structural refinement of the β-As_4S_4 crystallized after the thermal treatments (sample B) shows that this phase (Tables 2, 5, and 6) corresponds to the one reported by Porter and Sheldrick (1972). Its unit-cell volume has a slightly larger value (812.0 vs. 806.7 Å^3), with all axes *a*, *b*, and *c*, as well as the monoclinic angle β being larger. Small differences in the interatomic bond distances for the As3-S2, As3-S3, and As1-As2 are also noticeable. The results of the QPA for sample D shows that during the thermal treatment pararealgar transforms completely into the β-As_4S_4 and no amorphous phase occurs during the process. This phenomenon is even more difficult to be explained with the model proposed for realgar by Kyono et al. (2005) and, more generally, for arsenic sulfides by Bonazzi et al. (2006), since it should be presumed that a sulfur atom driven by heat should follow an opposite pattern than the one depicted in Figure 6 of Kyono et al. (2005). These authors explain the expansion of the unit-cell of realgar and β-As_4S_4, and its alteration to pararealgar by the increasing amount of As_4S_5 molecules forming in the structure, but that should be proportional to the amount of arsenolite produced, according to the before mentioned reaction. Without the formation of arsenolite, and taking into account the reversibility of the alteration of β-As_4S_4, as observed for sample D, the model is not suitable to explaining the process.

ACKNOWLEDGMENTS

We are grateful to Andrea Ienco for the help in XRPD data collection, Daniele Borrini for his help during the synthesis of the β-As_4S_4, and the two anonymous referees who provided useful suggestions. This work was founded by the research grant no. 21403(296) of the University of Florence.

REFERENCES CITED

Ballirano, P. and Maras, A. (2006) In-situ X-ray transmission powder diffraction study of the kinetics of the light-induced alteration of realgar (α-As_4S_4). European Journal of Mineralogy, 18, 589–599.

Bindi, L. and Bonazzi, P. (2007) Light-induced alteration of arsenic sulfides: A new product with an orthorhombic crystal structure. American Mineralogist, 92, 617–620.

Bindi, L., Popova, V., and Bonazzi, P. (2003) Uzonite, As_4S_5, from the type locality: single-crystal X-ray study and effects of exposure to light. Canadian Mineralogist, 41, 1463–1468.

Bonazzi, P. and Bindi, L. (2008) A crystallographic review of arsenic sulfides: effects of chemical variations and changes induced by exposure to light. Zeitschrift für Kristallographie, 223, 132–147.

Bonazzi, P., Menchetti, S., and Pratesi, G. (1995) The crystal structure of pararealgar, As_4S_4. American Mineralogist, 80, 400–403.

Bonazzi, P., Menchetti, S., Pratesi, G., Muniz-Miranda, M., and Sbrana, G. (1996) Light-induced variations in realgar and β-As_4S_4: X-ray diffraction and Raman studies. American Mineralogist, 81, 874–880.

Bonazzi, P., Bindi, L., Olmi, F., and Menchetti, S. (2003a) How many alacranites do exist? A structural study of non-stoichiometric As_8S_{9-x} crystals. European Journal of Mineralogy, 15, 282–288.

Bonazzi, P., Popova, V.I., Pratesi, G., and Menchetti, S. (2003b) Alacranite, As_8S_9: structural study of the holotype and re-assignment of the original chemical formula. American Mineralogist, 88, 1796–1800.

Bonazzi, P., Bindi, L., Pratesi, G., and Menchetti, S. (2006) Light-induced changes in molecular arsenic sulfides: State of the art and new evidence by single-crystal X-ray diffraction. American Mineralogist, 91, 1323–1330.

Burgio, L., Clark, R.J.H., and Theodoraki, K. (2003) Raman microscopy of Greek icons: identification of unusual pigments. Spectrochimica Acta, A, 59, 2371–2389.

Burgio, L., Clark, R.J.H., and Rosser-Owen, M. (2006) Raman analysis of ninth-century Iraqi stuccoes from Samarra. Journal of Archaeological Science, 34, 756–762.

Clark, R.J.H. and Gibbs, P.J. (1997) Identification of lead(II) sulfide and pararealgar on a 13th century manuscript by Raman microscopy. Chemical Communications, 11, 1003–1004.

——— (1998) Raman microscopy of a 13th-century illuminated text. Analytical Chemistry News & Features, 70, 99A–104A.

Corbeil, M.-C. and Helwig, K. (1995) An occurrence of pararealgar as an original or altered artists' pigment. Studies in Conservation, 40, 133–138.

de Vries, R.I., Weijers, S., Bethke, K., Kogan, V., Vasterink, J., Kharchenko, A., Fransen, M., and Bethke, J. (2007) Medipix 2 in X-ray diffraction. Nuclear Instruments and Methods in Physics Research, A, 576, 164–168.

Douglass, D.L., Shing, C., and Wang, G. (1992) The light-induced alteration of realgar to pararealgar. American Mineralogist, 77, 1266–1274.

Gualtieri, A.F. (2000) Accuracy of XRPD QPA using the combined Rietveld-RIR method. Journal of Applied Crystallography, 33, 267–278.

Hasapis, T.C., Hatzikraniotis, E., Paraskevopoulos, K.M., Andrikopoulos, K.S., Yannopoulos, S.N., and Wagner, T. (2010) Far infrared spectra of the AsS_2 and $AgAsS_2$ bulk glasses. Proceedings of the XXVI Conference on Solid State Physics and Materials Science, Ioannina, 132–133.

Ito, T., Morimoto, N., and Sadanaga, R. (1952) The crystal structure of realgar. Acta Crystallographica, 5, 775–782.

Kaban, I., Jóvári, P., Wágner, T., Bartoš, M., Frumar, M., Beuneu, B., Hoyer, W., Mattern, N., and Eckert, J. (2011) Structural study of AsS_2–Ag glasses over a wide concentration range. Journal of Non-Crystalline Solids, 357, 3430–3434.

Krbal, M., Wagner, T., Srba, T., Schwarz, J., Orava, J., Kohoutek, T., Zima, V., Benes, L., Kasap, S.O., and Frumar, M. (2007) Properties and structure of $Ag_x(As_{0.33}S_{0.67})_{100-x}$ bulk glasses. Journal of Non-Crystalline Solids, 353, 1232–1237.

Kutoglu, V.A. (1976) Darstellung und Kristallstruktur einer neuen isomeren Form von As_4S_4. Zeitschrift für Anorganische und Allgemeine Chemie, 419, 176–184.

Kyono, A. (2007) Experimental study of the effect of light intensity on arsenic sulfide (As_4S_4) alteration. Journal of Photochemistry and Photobiology A: Chemistry, 189, 15–22.

Kyono, A., Kimata, M., and Hatta, T. (2005) Light-induced degradation dynamics in realgar: in situ structural investigation using single-crystal X-ray diffraction study and X-ray photoelectron spectroscopy. American Mineralogist, 90, 1563–1570.

Larson, A.C. and Von Dreele, R.B. (2004) General Structure Analysis System

(GSAS). Los Alamos National Laboratory Report LAUR 86-748.

Lu, D.P., Qiu, J.Y., Jiang, B., Wang, Q., Liu, K.Y., Liu, Y.R., and Chen, S.S. (2002) Tetra-arsenic tetrasulfide for treatment of acute promyelocytic leukemia: a pilot report. Blood, 99, 3136–3143.

Mullen, D.J.E. and Nowacki, W. (1972) Refinement of the crystal structures of realgar, AsS and orpiment, As_2S_3. Zeitschrift für Kristallographie, 136, 48–65.

Muniz-Miranda, M., Sbrana, G., Bonazzi, P., Menchetti, S., and Pratesi, G. (1996) Spectroscopic investigation and normal mode analysis of As_4S_4 polymorphs. Spectrochimica Acta, A, 52, 1391–1401.

Naumov, P., Makreski, P., and Jovanovski, G. (2007) Direct atomic scale observation of linkage isomerization of As_4S_4 clusters during the photoinduced transition of realgar to pararealgar. Inorganic Chemistry, 46, 10624–10631.

Porter, E.J. and Sheldrick, G.M. (1972) Crystal structure of a new crystalline modification of tetra-arsenic tetrasulphide (2,4,6,8-tetrathia-1,3,5,7-tetraarsatricyclo[3,3,0,0]-octane). Journal of the American Chemical Society Dalton, 13, 1347–1349.

Roland, G.W. (1972) Concerning the α-AsS ↔ realgar inversion. Canadian Mineralogist, 11, 520–525.

Stephens, P.W. (1999) Phenomenological model of anisotropic peak broadening in powder diffraction. Journal of Applied Crystallography, 32, 281–289.

Street, B.G. and Munir, Z.A. (1970) The structure and thermal properties of synthetic realgar (As4S4). Journal of Inorganic Nuclear Chemistry, 32, 3769–3774.

Toby, B.H. (2001) EXPGUI, a graphical user interface for GSAS. Journal of Applied Crystallography, 34, 210–213.

Trentelman, K., Stodulski, L., and Pavlosky, M. (1996) Characterisation of pararealgar and other light-induced transformation products from realgar by Raman microspectroscopy. Analytical Chemistry, 68, 1755–1761.

Wágner, T., Krbal, M., Kohoutek, T., Peøina, V., Vlček, Mir., Vlček, Mil., and Frumar, M. (2003) Kinetics of optically- and thermally-induced diffusion and dissolution of silver in spin-coated $As_{33}S_{67}$ amorphous films; their properties and structure. Journal of Non-Crystalline Solids, 326 and 327, 233–237.

Xiong, X.X. and Liu, C.T. (1998) Mineralogical study of realgar from the Shimen As(Au) deposit, Hunan province. Acta Petrologica et Mineralogica, 378–384.

Zhao, Q.H., Zhang, Y., Liu, Y., Wang, H.L., Shen, Y.Y., Yang, W.J., and Wen, L.P. (2009) Anticancer effect of realgar nanoparticles on mouse melanoma skin cancer *in vivo* via transdermal drug delivery. Medical Oncology, 27, 203–212.

Zoppi, M. (1998) Alterazione indotta dalla luce sul minerale realgar. Tesi di Laurea, Dipartimento di Scienze della Terra, Università degli Studi di Firenze.

Manuscript received August 11, 2011
Manuscript accepted January 4, 2012
Manuscript handled by Oliver Tschauner